

# FRICITION FORCES AND FRICTION COEFFICIENT IN SLIDE PARABOLIC MICRO-BEARING WITH CONSIDERATION OF THE ADHESION FORCE

**Andrzej Miszczak**

*Maritime University Gdynia, Faculty of Marine Engineering  
Morska Street 83, 81 225 Gdynia, Poland  
tel.: +48 58 6901348, fax: +48 58 6901399  
e-mail: miszczak@am.gdynia.pl*

**Adam Czaban**

*Maritime University Gdynia, Faculty of Marine Engineering  
Morska Street 83, 81 225 Gdynia, Poland  
tel.: +48 58 6901304, fax: +48 58 6901399  
e-mail: aczaban@am.gdynia.pl*

## **Abstract**

*Micro-bearings have many applications in computer devices, such as CPU fans or hard disc drives. So far, rolling bearings and slide bearings have been used, for example micro-bearing with smooth journal and sleeve surface, which is known as FDB - Fluid Dynamic Bearing. Actually, latter versions of micro-bearings are being launched to the market: Ex-FDB - Extra Fluid Dynamic Bearing. This type of bearings was fabricated by putting some micro-grooves filled with oil on its internal surfaces. Ex-FDB's are characterized by reduced level of generated noise and guarantee long failure-free fan life, reaching 120 000 hours.*

*In this paper we present our numerical calculations of the friction force and the friction coefficient in the parabolic micro-bearing.*

*Micro-bearing gap height is very low, often less than 1 micrometer, therefore capillarity and adhesion forces cause an increase of oil viscosity near the journal and sleeve surfaces. Due to this fact a value of hydrodynamic pressure in micro-bearing gap also increases, what results in observed changes of capacity, friction forces and friction coefficient values.*

*The influence of adhesion and capillarity on friction force and friction coefficient of oil in micro-bearing hasn't been considered from analytical point of view so far.*

*This paper presents numerical results of computed values of friction forces and friction coefficient for parabolic micro-bearing in comparison to values for classical parabolic bearing.*

**Keywords:** *adsorption, adhesion, capillary forces, micro-bearing lubrication*

## **1. Introduction**

Slide micro-bearings are finding more and more applications. A classic example is the slide bearings in fans of computers and HDD drives. Another example of pneumatic slide micro-bearings is dental contra-angle handpieces. Slide micro-bearings used in HDD drives and fans are designated with a symbol, FDB – Fluid Dynamic Bearing. Currently, newer versions of the sliding micro-bearings are put on the market, known as Extra Fluid Dynamic Bearing (Ex-FDB).

Sliding micro-bearings most frequently work at high rotational speeds from a few to tens of revolutions per minute at low loads.

In this paper, the authors will present the results of numerical calculations of distribution of hydrodynamic pressure, capacity force, friction force and friction coefficient in a parabolic slide micro-bearing, lubricated using classic oil, considering the adhesion forces that occur in super thin

boundary layers [1, 3-7, 12].

The aim of this study is to compare the value of the load-bearing forces, friction forces and coefficients of friction occurring in a parabolic sliding micro-bearing lubricated with classic oil, considering changes in viscosity from adhesion forces with the values of load-bearing forces, friction forces and friction coefficients obtained in numerical calculations when changes of viscosity from adhesion forces are not taken into account.

An equation describing the change in hydrodynamic pressure has been derived analytically from the basic motion equations, i.e. the momentum conservation equation, the equation of stream continuity after the appropriate boundary conditions have been applied [8-11].

For analytical and numerical calculations, laminar steady flow of lubricant is assumed, with classical Newtonian properties.

The geometry of the micro-bearing journal with a parabolic surface including depressions is shown in Fig. 1.

The slot of a modern sliding micro-bearing differs significantly from a classic slide bearing slot, as it is incised with micro or nanodepressions with various shapes. Most often, the shape is that of a herringbone or a spiral [2]. Also considered are groove-shaped depressions arranged axially or peripherally [10, 11].

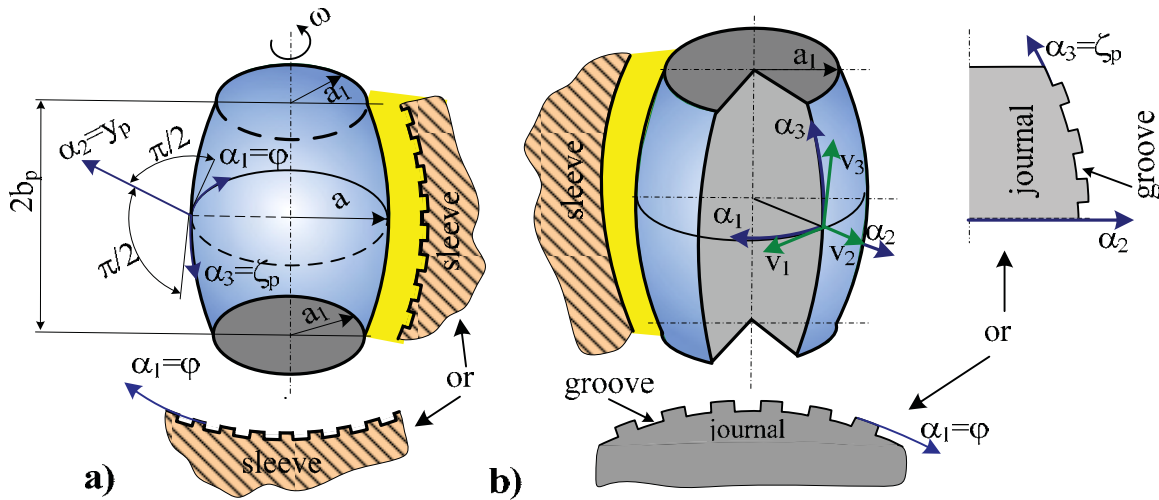


Fig. 1. Parabolic journal for hydrodynamic micro-bearing: a) circumferential or longitudinal grooves on the parabolic sleeve, b) longitudinal or circumferential grooves on the parabolic journal

The mathematical equation describing such a slot can be written down in the following form [10]:

$$\varepsilon_T(\varphi, \zeta_p, t) = \varepsilon \left[ 1 + \lambda_h(\zeta_p, t) \cos \varphi + \varepsilon_{g1} \sum_{n=0}^k (-1)^n H_n(\varphi - 0.5n\varphi_T) \right], \quad (1)$$

$$\varepsilon_T(\varphi, \zeta_p, t) = \varepsilon \left[ 1 + \lambda_h(\zeta_p, t) \cos \varphi + \varepsilon_{g1} \sum_{n=0}^k (-1)^n H_n(\zeta_p - 0.5n\zeta_T) \right],$$

where:

$$0 \leq \varphi < 2\pi, \quad -b_p \leq \zeta_p \leq b_p,$$

$\varepsilon_{g1} \equiv \varepsilon_g / \varepsilon$ ,  $\varepsilon_g$  - groove height,

$\lambda_p$  - relative eccentricity,

$\varepsilon$  - micro-bearing radial clearance,

$H_n$  - heaviside function,

$\varphi_T, \zeta_T$  - values that specify the period of depressions.

The present study also includes dynamic viscosity changes resulting from the impact of adhesion forces in a super-thin layer of lubricant. The dynamic viscosity of the oil lubricating the slide micro-bearing is then the sum of classical viscosity and viscosity resulting from the effects of adhesion forces. The value of the total dynamic viscosity is determined from the following relationship:

$$\eta(\varphi, y_p, \zeta_p) = \eta_o \left[ 1 + a_\eta k + \frac{b_\eta}{\varepsilon_T} \left( e^{c_\eta y_p^2 - d_\eta y_p + f_\eta} \right) \right], \quad (2)$$

where:

k - curvature (the inverse of the radius of curvature),

$a_\eta, b_\eta, c_\eta, d_\eta, f_\eta$  - experimental coefficients,

$\eta_o$  - characteristic dimensional value of dynamic viscosity.

## 2. Distribution of hydrodynamic pressure in a sliding micro-bearing slot

For a parabolic sliding micro-bearing, we assume the following indicators of curvilinear coordinates:  $\alpha_1 = \varphi, \alpha_2 = y_p, \alpha_3 = \zeta_p$ . These coordinates are shown in Fig. 1. In addition, the following indications for the journal have been assumed:  $a_1$  - smallest radius of the parabolic journal,  $a$  - largest radius of the parabolic journal,  $2b_p$  - bearing length.

The Reynolds-type equation based on which the distribution of hydrodynamic pressure was determined by the authors through solving equations of motion, i.e. the momentum equation and the stream continuity equation. These equations were solved in a parabolic coordinate system, using simplifications characteristic of a thin boundary layer and corresponding boundary conditions. The modified Reynolds equation for a parabolic slide micro-bearing has the following form [10]:

$$\begin{aligned} \frac{\partial}{\partial \varphi} \left[ \left( \frac{\partial p}{\partial \varphi} + \frac{\partial p_{adh}}{\partial \varphi} \right) \int_0^{\varepsilon_T} A_\eta dy_p \right] + \frac{h_\varphi}{h_\zeta} \frac{\partial}{\partial \zeta_p} \left[ \frac{h_\varphi}{h_\zeta} \left( \frac{\partial p}{\partial \zeta_p} + \frac{\partial p_{adh}}{\partial \zeta_p} \right) \int_0^{\varepsilon_T} A_\eta dy_p \right] = \\ = \omega h_\varphi^2 \frac{\partial}{\partial \varphi} \left[ \int_0^{\varepsilon_T} A_s dy_p - \varepsilon_T \right] + h_\varphi^2 \frac{\partial \varepsilon_T}{\partial t}, \end{aligned} \quad (3)$$

where:

$$A_s(\varphi, y_p, \zeta_p, t) \equiv \frac{\int_0^{y_p} \frac{1}{\eta + \eta_{adh}} dy_p}{\int_0^{\varepsilon_T} \frac{1}{\eta + \eta_{adh}} dy_p},$$

$$A_\eta(\varphi, y_p, \zeta_p, t) \equiv \int_0^{y_p} \frac{y_p}{\eta + \eta_{adh}} dy_p - A_s(\varphi, y_p, \alpha_3, t) \int_0^{\varepsilon_T} \frac{y_p}{\eta + \eta_{adh}} dy_p, \quad (4)$$

where:

$0 \leq y_p \leq \varepsilon_T, 0 \leq \varphi < 2\pi\theta_1, 0 \leq \theta_1 < 1$  and  $-b_p \leq \zeta_p \leq b_p$  for parabolic journal,

$\varepsilon_T(\varphi, \zeta_p, t)$  - the total height gap,

$p_{adh}$  - hydrodynamic pressure changes resulting from allowing for adhesion,

$\eta = \eta(\varphi, \zeta_p)$  - dynamic viscosity,

t - time,

For the parabolic journal shape of the sliding micro-bearing, we have the following coefficients:

$$h_\varphi = a \cos^2(\Lambda_{p1} \zeta_{p1}), \quad h_\zeta = \sqrt{1 + 4(\Lambda_{p1} / L_{p1})^2 \sin^2(\Lambda_{p1} \zeta_{p1})} \cos(\Lambda_{p1} \zeta_{p1}), \quad (5)$$

$$\Lambda_{p1} \equiv \sqrt{\frac{a - a_1}{a}}, \quad L_{p1} \equiv \frac{b_p}{a}, \quad \zeta_{p1} \equiv \frac{\zeta_p}{b_p}.$$

### 3. Friction forces and friction coefficients for the parabolic micro-bearing

The friction force components in the direction of the  $\varphi$  and  $\zeta_p$  coordinates are determined based on the following known relationships:

$$F_{R\varphi} = \iint_{\Omega} \left[ (\eta + \eta_{adh}) \frac{\partial v_\varphi}{\partial y_p} \right]_{y_p = \varepsilon_T} h_\varphi h_\zeta d\varphi d\zeta_p, \quad F_{R\zeta} = \iint_{\Omega} \left[ (\eta + \eta_{adh}) \frac{\partial v_\zeta}{\partial y_p} \right]_{y_p = \varepsilon_T} h_\varphi h_\zeta d\varphi d\zeta_p, \quad (6)$$

where:

$\Omega$  - lubrication surface,

$v_\varphi, v_\zeta$  - dimensional velocity components in the direction of  $\varphi, \zeta_p$ .

By substituting the respective functions of the velocity vector components [10] to the formula (11) and then simplifying it, we obtain the following forms of equations for the circumferential peripheral component  $F_{R\varphi}$  and longitudinal  $F_{R\zeta}$  of the friction force:

$$F_{R\varphi} = \iint_{\Omega} \left[ \frac{\eta + \eta_{adh}}{h_\varphi} \left( \frac{\partial p}{\partial \varphi} + \frac{\partial p_{adh}}{\partial \varphi} \right) \frac{\partial A_\eta(\varphi, y_p, \zeta_p)}{\partial y_p} \right]_{y_p = \varepsilon_T} h_\varphi h_\zeta d\varphi d\zeta_p +$$

$$- \iint_{\Omega} \left[ \omega h_\varphi (\eta + \eta_{adh}) \frac{\partial A_s(\varphi, y_p, \zeta_p)}{\partial y_p} \right]_{y_p = \varepsilon_T} h_\varphi h_\zeta d\varphi d\zeta_p, \quad (7)$$

$$F_{R\zeta} = \iint_{\Omega} \left[ \frac{\eta + \eta_{adh}}{h_\zeta} \left( \frac{\partial p}{\partial \zeta_p} + \frac{\partial p_{adh}}{\partial \zeta_p} \right) \frac{\partial A_\eta(\varphi, y_p, \zeta_p)}{\partial y_p} \right]_{y_p = \varepsilon_T} h_\varphi h_\zeta d\varphi d\zeta_p. \quad (8)$$

The coefficient of friction is derived from the following relationship:

$$\mu_p = \frac{\sqrt{(F_{R\varphi})^2 + (F_{R\zeta})^2}}{C_{tot}^{(p)}}, \quad (9)$$

where:

$C_{tot}$  - capacity force for the parabolic sliding bearing.

### 4. Numerical calculations

Numerical calculations of the distribution of hydrodynamic pressure, capacity force, friction force and coefficient of friction were performed using Mathcad 14 and own calculation procedures based on the finite difference method. In the first place, pressure distributions were determined using partial differential equation (3). Calculations were performed using the Reynolds boundary condition. The numerical integration area was contained within the following limits:  $0 \leq \varphi \leq \varphi_k$ ,  $-b_p \leq \zeta_p \leq b_p$ . The height gap was assumed for the numerical calculations in the following form:

$$\varepsilon_T = \varepsilon(1 + \lambda_p \cos \varphi), \quad (10)$$

where:

$\lambda_p$  - relative eccentricity,

$\varepsilon$  - radial clearance.

Figure 2 presents the results of numerical calculations of hydrodynamic pressure distribution for the relative eccentricity  $\lambda=0.4$  and  $\lambda=0.6$  and the following calculation: smallest radius of the journal  $a_1=0.0012$  m, largest radius of the journal  $a=0.0015$  m, relative radial clearance  $\psi=0.003$ , radial clearance  $\varepsilon=2 \cdot 10^{-6}$  m, bearing length  $2b_p=0.003$ m, bearing dimensionless length  $L_{p1}=b_p/a=1$ , lubricating oil dynamic viscosity  $\eta=0.020$  Pas, the surface curvature coefficient  $k=1000$  m<sup>-1</sup>, angular velocity  $\omega=754$  s<sup>-1</sup>, experimental factors including the impact of adhesion on viscosity change:  $a_\eta=0.000040$  m,  $b_\eta=0.000001$  m,  $c_\eta=22.222222$  m<sup>-2</sup>,  $d_\eta=33.333333$  m<sup>-1</sup>,  $f_\eta=12.500000$ , characteristic dimensional value of hydrodynamic pressure  $p_0=\omega\eta R^2/\varepsilon^2$ ,  $p_0=1.675$  MPa.

Figures 2a and 2c present the distributions of hydrodynamic pressure in the parabolic sliding micro-bearing slot lubricated using classic Newtonian oil without taking into account changes in viscosity from adhesion forces.

Figures 2b and 2d present the distributions of hydrodynamic pressure in the parabolic sliding micro-bearing slot lubricated using classic Newtonian oil taking into account changes in viscosity from adhesion forces.

The values of the capacity forces and friction forces for the eccentricity ratio  $\lambda_p=0.1$  to  $\lambda_p=0.9$  considering changes of viscosity from adhesion forces, and without considering them are shown in Fig. 3 and 4.

If the eccentricity ratio varies from  $\lambda_p=0.1$  to  $\lambda_p=0.9$ , the maximum values of hydrodynamic pressure vary from 0.4 MPa to 110.7 MPa and the aerodynamic lift acting in the direction of the  $y_p$  axis varies from 1.78 N to 196.80 N.

For the numerical calculations presented, the end of the oil film, with the Reynolds boundary condition, is located, respectively from  $\varphi_k=3.794$  rad from  $\varphi_k=3.418$ , with a suitably changing eccentricity ratio from  $\lambda_p=0.1$  to  $\lambda_p=0.9$ .

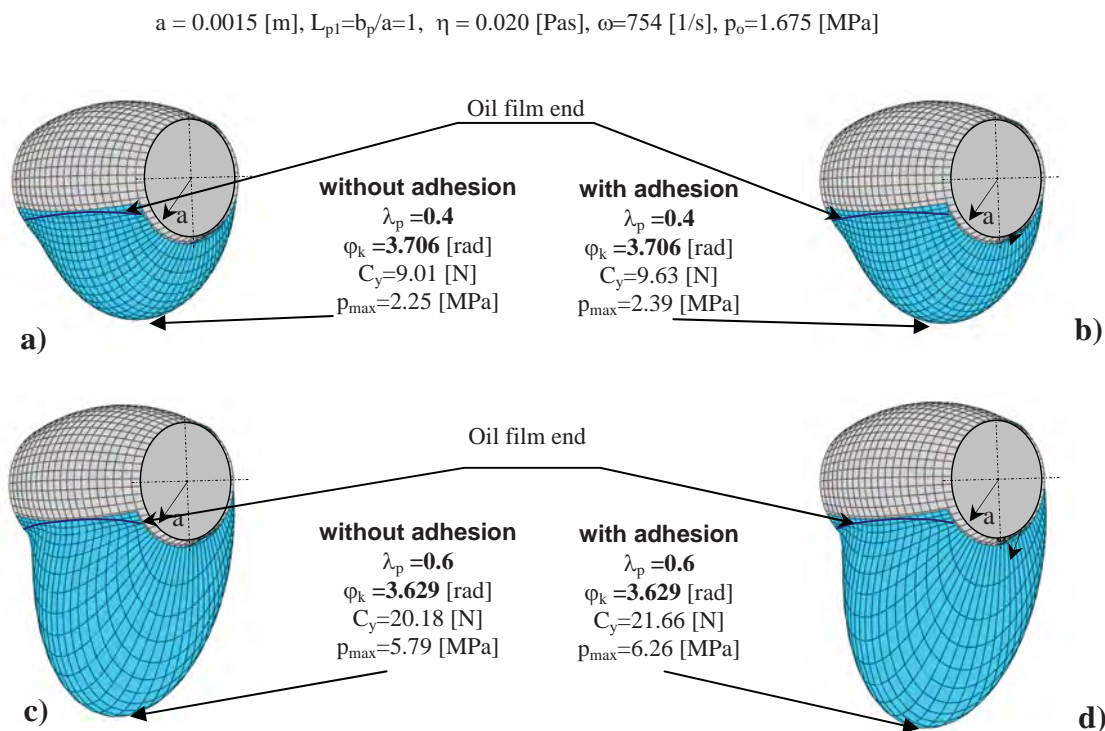


Fig. 2. The pressure distributions in hyperbolic micro-bearings caused by the rotation in circumferential direction: a) without influences of adhesion forces on the oil viscosity, b) with viscosity changes caused by the adhesion

The friction coefficient values calculated using formula (9) are shown in Fig. 5. The values are also calculated considering changes of viscosity from adhesion forces and passing over the influences.

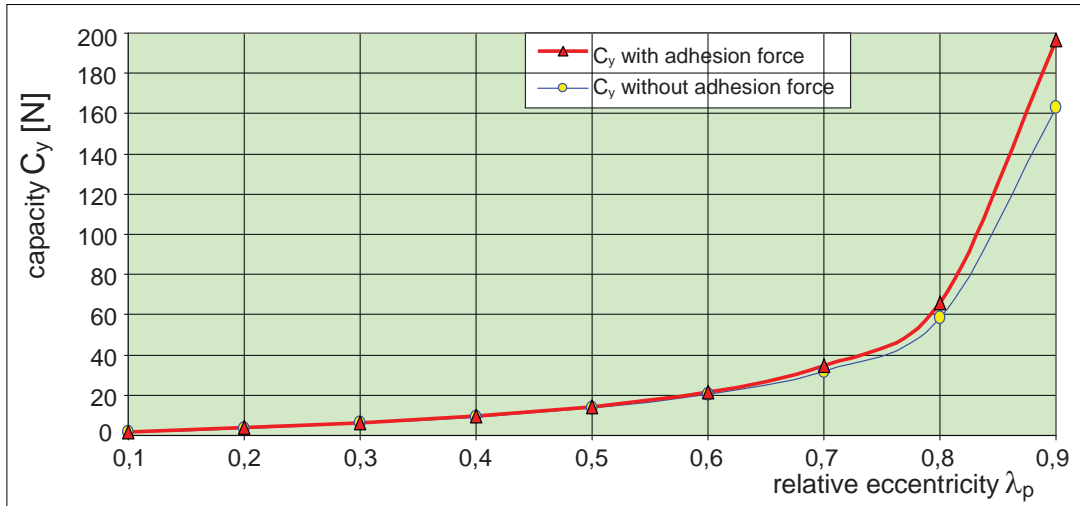


Fig. 3. The capacity force  $C_y$  with and without adhesion force influences

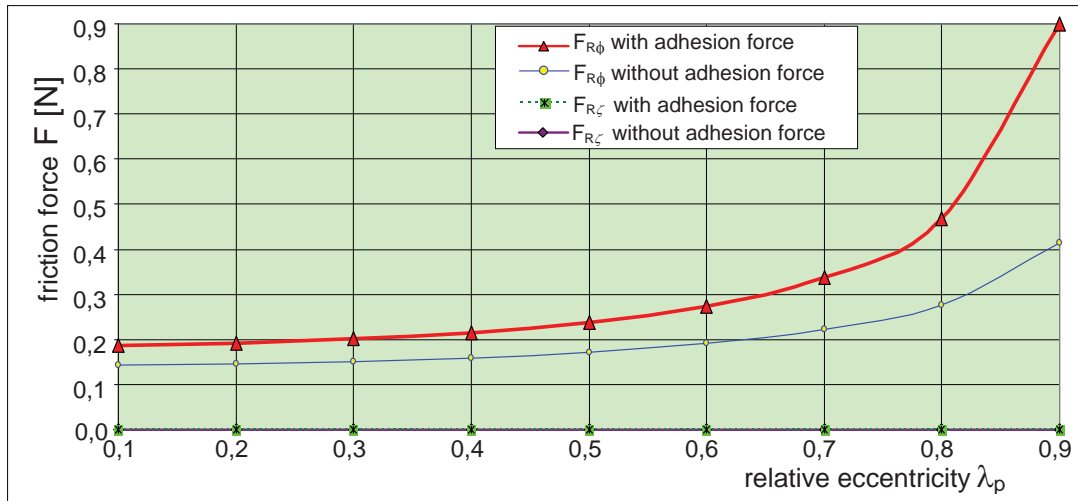


Fig. 4. The friction force components  $FR\phi$ ,  $FR\zeta$  with and without adhesion force influences

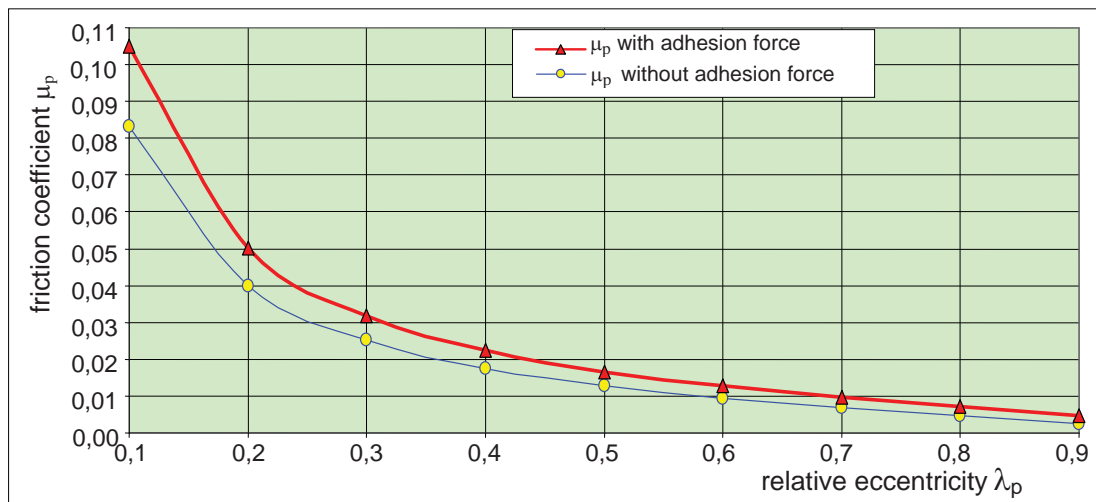


Fig. 5. The friction coefficient  $\mu_p$  with and without adhesion force influences

## 5. Observations and conclusions

1. Longitudinal component of friction force in a parabolic sliding micro-bearing is minimal.
2. Dynamic viscosity changes resulting from taking adhesion forces into account result in an increase in the aerodynamic force in the sliding micro-bearing. For an eccentricity ratio of  $\lambda_p=0.1$  to  $\lambda_p=0.9$ , the aerodynamic force increases from 4% to 21%, respectively, compared to the value of the aerodynamic force without considering the influence of adhesion.
3. Dynamic viscosity changes resulting from taking adhesion forces into account result in an increase in the friction force in the parabolic sliding micro-bearing. For an eccentricity ratio of  $\lambda_p=0.1$  to  $\lambda_p=0.9$ , the friction force increases from 31% to 118%, respectively, compared to the value of the friction force without considering the influence of adhesion.
4. A similar situation is observed for the coefficient of friction. For an eccentricity ratio of  $\lambda_p=0.1$  to  $\lambda_p=0.9$ , the friction factor increases from 26% to 80%, respectively, compared to the value of the friction factor without considering the influence of adhesion.

## References

- [1] Eui-Sung Yoon, Seung Ho Yang, Hung-Gu Han, Hosung Kong, *An experimental study on the adhesion at a nano-contact*, *Wear*, 254, pp. 974-980, 2003.
- [2] Jang, G. H., Lee, S. H., Kim, H. W., Kim, C. S., *Dynamic analysis of a HDD spindle system with FDBs due to the bearing width and asymmetric grooves of journal bearing* . Microsystems Technologies, 11, pp. 499-505, 2005.
- [3] Kogut, L., Etsion, I., *Adhesion in elastic-plastic spherical microcontact* , *Journal of Colloid and Interface Science*, 261, pp. 372-378, 2003.
- [4] Manabu Takeuchi, *Adhesion Forces of Charged Particles*, *Chemical Engineering Science*, 61, pp. 2279-2289, 2006.
- [5] Miranda, J. A., Oliveira, R. M., *Adhesion phenomena in ferrofluids* , *Physical Review E*, 70, pp. 1-11, 2004.
- [6] Rymuza, Z., Kusznierevich, Z., Solarski, T., Kwacz, M., Chizhik, S., Goldade, A. V., *Static friction and adhesion in polimer-polymer micro-bearings*, *Wear*, 238, pp. 56-69, 2000.
- [7] Taylor, C. J., Dieker, L. E., Miller, K. T., Koh, C. A., Dendy, S. E., *Micromechanical adhesion force measurements between tetrahydrofuran hydrate particles* , *Journal of Colloid and Interface Science*, 306, pp. 255-261, 2007.
- [8] Wierzcholski, K., Miszczak, A., *A study on the adhesion at a micro and nano lubrication*, *Journal of Kones Powertrain and Transport*, Vol. 16, No. 4, pp. 499-506, Warsaw 2009.
- [9] Wierzcholski, K., Miszczak, A., *Adhesion and capilarity in micro- bearing lubrication* , *Journal of Kones Powertrain and Transport*, Vol. 16, No. 3, pp. 497-504, Warsaw 2009.
- [10] Wierzcholski, K., *Adhesion and cohesion forces occurring in parabolical microbearing* , *Tribologia*, 5 (227), pp. 221-228, 2009.
- [11] Wierzcholski, K., *Adhesion influences on the pressure and carrying capacity of cylindrical microbearing*, *Tribologia*, 5 (227), pp. 229-236, 2009.
- [12] Zhou, H., Goetzinger, M., Peukert, W., *The influence of particle charge and roughness on particle-substrate adhesion*, *Powder Technology*, 135-136, pp. 82-91, 2003.